JOURNAL OF SOLID STATE CHEMISTRY **127,** 151–160 (1996)
ARTICLE NO. 0371

Synthesis and Characterization of Quaternary Sulfides with $ThCr_2Si_2$-Type Structure: $KCo_{2-x}Cu_xS_2$ ($0.5 \leq x \leq 1.5$) and $ACoCuS_2$ (A = K, Rb, Cs)

M. Oledzka, J.-G. Lee, K. V. Ramanujachary,[1] and M. Greenblatt[2]

Department of Chemistry, Rutgers, the State University of New Jersey, P.O. Box 939, Piscataway, New Jersey 08855–0939

Received April 16, 1996; in revised form August 19, 1996; accepted August 22, 1996

Synthesis, electrical, and magnetic properties of new quaternary alkali metal mixed-transition metal sulfides [$ACoCuS_2$ (A = K, Rb, Cs) and $KCo_{2-x}Cu_xS_2$ ($0.5 \leq x \leq 1.5$)] are reported. The synthesis was accomplished by sulfurization of a mixture of corresponding alkali metal carbonate and copper and cobalt oxides. All of the phases form in the tetragonal $ThCr_2Si_2$-type structure in space group $I4/mmm$. The electrical resistivity measurements show that the new phases are semiconducting, with room temperature resistivities $\rho_{RT} \sim 10^{-2}\ \Omega \cdot$ cm; $KCo_{0.5}Cu_{1.5}S_2$ is metallic with a metal-to-nonmetal transition at ~120 K. Seebeck measurements indicate that the majority of charge carriers are holes. The temperature dependence of magnetic susceptibility shows an anomalous transition to the ferromagnetic state in the $ACoCuS_2$ phases. The electrical and magnetic properties of the new quaternary phases are compared with those of ternary ACo_2S_2 (A = K, Rb, Cs).

INTRODUCTION

More than 400 compounds of AM_2X_2 stoichiometry are known to adopt the $ThCr_2Si_2$-type structure, where A typically is a rare earth, alkaline earth, or alkali metal ion, M is a transition metal or a main group element, and X usually is from group 13, 14, or 15 (1). The $ThCr_2Si_2$-type structure is an example of a two-dimensional (2D) layered structure shown in Fig. 1. The layers are built of edge-sharing MX_4 tetrahedra extended two dimensionally in the ab plane. The M–X distance is equal to the sum of the covalent radii of M and X. The A ions, coordinated by eight X ions, are between two layers of the infinite sheets of MX_4 tetrahedra, and the A–X distance is close to the sum of the ionic radii of A and X. The relatively short M–M distance within one layer (e.g., 2.65 Å for $TlCo_2S_2$) indicates the possibility of metal–metal bonding (2). Compounds with layered 2D or chain (one-dimensional, 1D) structures are known as low-dimensional (LD) compounds and provide a class of materials that may exhibit unusual physical properties. Electronic correlations in LD metals often lead to interesting instabilities such as metal–insulator (MI) transitions, superconductivity, or charge-density waves (CDWs) [e.g., Refs. (3, 4)]. Accordingly, materials that adopt the $ThCr_2Si_2$-type structure have been the subject of numerous investigations (5). It is interesting that only about 20 ternary chalcogenides and some of their solid solutions (6) as well as nine quaternary sulfides with the $ThCr_2Si_2$-type structure have been reported so far (7–9). Transition metal sulfides with LD structures have been studied extensively in recent years, partly because of their similarity to the high-temperature copper oxide superconductors (10). This includes especially the high degree of covalency of the M–S bond (where M is a first-row transition metal), which is similar to that of the Cu–O bond, and the layered 2D structure (11).

The ternary cobalt chalcogenides with the formula ACo_2S_2 (where A = K, Rb, Cs, Tl; X = S, Se) investigated in our laboratory belong to this group of compounds with the $ThCr_2Si_2$-type structure (6). These chalcogenides are ferromagnetic metallic conductors, except for $TlCo_2Se_2$ and $CsCo_2Se_2$, which are also metallic, but order antiferromagnetically.

Another member of this group is the potassium intercalate of the chalcopyrite, $KCuFeS_2$, reported by Mujica *et al.* (7), which to our knowledge is the first alkali metal mixed-transition metal quaternary sulfide with the $ThCr_2Si_2$-type structure. The isostructural mineral murunskite reported in 1980 has the composition $K_2Cu_3FeS_4$ ($KCu_{1.5}Fe_{0.5}S_2$) (12). Single-crystal X-ray diffraction studies show that in $KCuFeS_2$ both Cu and Fe ions occupy the same crystallographic site, i.e., the centers of the S_4 tetrahedra in the layer formed by edge-sharing MS_4 tetrahedra. The potassium ions are between the layers of edge-sharing tetrahedra (Fig. 1) (7).

Based on these data we have examined the possibility of the formation of other mixed-transition metal sulfides

[1] Current address: Chemistry Department, Rowan College of New Jersey, Glassboro, NJ 08028–1701.

[2] To whom correspondence should be addressed.

0022-4596/96 $18.00

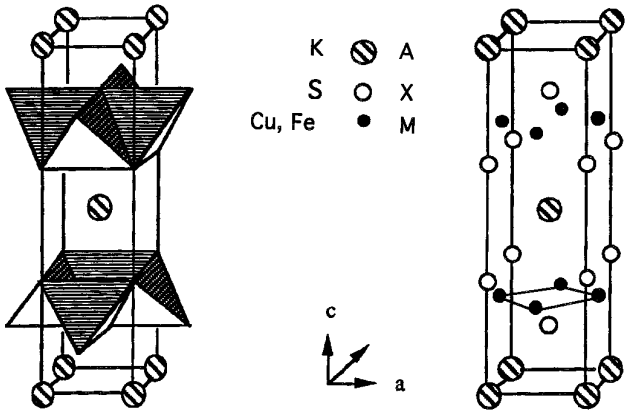

FIG. 1. Unit cell of AM_2X_2 ($KCuFeS_2$) with the $ThCr_2Si_2$ structure with and without the two-dimensional layers of MX_4 tetrahedra.

with the $ThCr_2Si_2$-type structure. We have focused on the system A–Co–Cu–S (where A = K, Rb, Cs), because ternary sulfides ACo_2S_2 with the $ThCr_2Si_2$-type structure have been already reported (see above) and we assumed that it might be possible to substitute some of the cobalt cations with copper cations to obtain quaternary metal sulfides with potentially interesting properties.

In this paper we report the synthesis and characterization of new phases: $ACoCuS_2$ (where A = K, Rb, Cs) and a series of new copper-substituted potassium cobalt sulfides $KCo_{2-x}Cu_xS_2$ ($0.5 \leq x \leq 1.5$), crystallizing in the $ThCr_2Si_2$-type structure.

EXPERIMENTAL

Initial synthetic efforts for $KCo_{2-x}Cu_xS_2$ included the use of reactive polysulfide flux K_2S_x. The potassium polysulfide flux, however, severely attacked the walls of quartz tubes, which significantly limited the amount of product that could be obtained. Therefore, the sulfurization method was chosen over the reactive flux method as a more effective way to synthesize those sulfides.

All of the reagents used were at least 99.9% pure. The synthesis was accomplished by sulfurization in a stream of CS_2 carried by N_2 gas. The starting materials—corresponding alkali metal carbonate, cobalt oxide, and copper oxide—were mixed in an agate mortar in a stoichiometric ratio and pressed into pellets. The pellets were placed in an alumina boat in a tube furnace in a CS_2/N_2 atmosphere at temperatures in the range 650–900°C for about 48 h with intermittent grindings. For some compositions, additional grindings followed by repelletization and reheating in a CS_2/N_2 atmosphere were necessary to obtain a homogeneous phase. The purity of the final products was examined by powder X-ray diffraction (PXD) analysis. The composition of the samples was determined by inductively coupled plasma emission spectroscopy (ICP) using a microprocessor-controlled Perkin Elmer Plasma 400 ICP spectrometer. The PXD data were collected with a SCINTAG PAD V diffractometer with Cu$K\alpha$ radiation in the 2Θ range 10° to 60°, using either KCl or Si powder as an internal standard. Because all the as-synthesized samples were air and moisture sensitive, the slides for the X-ray diffraction analysis were prepared in a glove box and the sample was protected by a polyethylene foil. The unit cell parameters were refined by a least-squares program. For transport measurements powder samples were pressed into pellets and sintered at ~700°C. The dc resistivity measurements were carried out by a standard four-probe technique with a closed-cycle cryostat (APD Cryogenics, DE 202) from room temperature to 30 K. Ohmic contacts were made by attaching molten indium ultrasonically to four spots of conducting silver paste on the sides of a brick-shaped polycrystalline pellet in a stream of an inert gas. Seebeck measurements were used to determine the nature of primary charge carriers (i.e., n or p type). Magnetic susceptibility of the samples was measured with a SQUID magnetometer (MPMS, Quantum Design) in an applied field of 1000 G in the temperature range 2–380 K.

RESULTS AND DISCUSSION

Synthesis and Structural Aspects

A series of new sulfides $KCo_{2-x}Cu_xS_2$ with $0.5 \leq x \leq 1.5$ were prepared. For samples with $x > 1.5$, a structurally related phase KCu_4S_3 (13) formed along with $KCo_{2-x}Cu_xS_2$. The synthesis, by a sulfurization method, of the end members of the series, i.e., KCo_2S_2 and KCu_2S_2, as well as samples with $x < 0.5$, was unsuccessful. The synthesis of KCo_2S_2 by a conventional solid-state technique has been already reported by Huan *et al.* (6). In contrast, KCu_2S_2 has not been reported to date and we were unable to prepare it either by a flux method or by solid state synthesis.

$RbCoCuS_2$ and $CsCoCuS_2$ were synthesized for the first time in the same way as their potassium analog. All of the sulfides prepared in this study are black and air and moisture sensitive. Prolonged exposure to air results in their decomposition.

The PXD patterns confirmed that the products were monophasic. As a further check of the purity of the synthesized compounds, the chemical composition of the $KCo_{2-x}Cu_xS_2$ series (x = 0.5, 0.75, 1.00, 1.20, 1.40, 1.50) was determined by the ICP method. As shown in Table 1, the composition of the products does not deviate significantly from the nominal starting composition; the lack of a distinctive trend in these small differences may indicate that the composition for each sample depends on the details of the synthesis. Because the Rb and Cs analogs of $KCoCuS_2$ were prepared under similar experimental conditions, we

TABLE 1
Results of the Elemental Analysis of $KCo_{2-x}Cu_xS_2$

Composition	K (wt%)	Co (wt%)	Cu (wt%)	S (wt%)
$KCo_{1.50}Cu_{0.50}S_2$				
Experimental	14.1(3)[a]	37.8(11)	15.7(10)	32.4[b]
Calculated	17.5	39.6	14.2	28.7
$KCo_{1.25}Cu_{0.75}S_2$				
Experimental	15.8(4)	32.4(2)	21.8(7)	30.1
Calculated	17.4	32.8	21.2	28.6
$KCoCuS_2$				
Experimental	16.4(10)	24.9(4)	28.8(6)	29.9
Calculated	17.3	26.1	28.2	28.4
$KCo_{0.80}Cu_{1.20}S_2$				
Experimental	18.8(11)	21.4(5)	36.6(2)	23.1
Calculated	17.3	20.8	33.7	28.3
$KCo_{0.60}Cu_{1.40}S_2$				
Experimental	16.4(7)	16.1(4)	39.7(7)	27.7
Calculated	17.2	15.5	39.1	28.2
$KCo_{0.50}Cu_{1.50}S_2$				
Experimental	16.1(7)	13.4(3)	40.8(9)	29.4
Calculated	17.2	12.9	41.8	28.1

[a] Numerical values in parentheses are the standard deviations.
[b] Sulfur content determined by weight difference.

assume that for these compounds the actual composition is not likely to deviate significantly from the nominal one.

The X-ray scattering factors of cobalt and copper atoms are similar and therefore any crystallographic ordering of these two types of atoms would be difficult to distinguish by PXD. In addition, we have found no evidence of superstructure reflections in any of the PXD patterns. Most probably, both atoms occupy the same crystallographic site randomly at the centers of S_4 tetrahedra, as in $KCuFeS_2$.

The PXD patterns for all new phases can be indexed based on a tetragonal unit cell (space group $I4/mmm$). A typical PXD pattern of a $KCo_{2-x}Cu_xS_2$ compound is shown in Fig. 2a. The PXD patterns for $RbCoCuS_2$ and $CsCoCuS_2$, are presented in Figs. 2b and 2c, respectively. The results of the cell parameter refinements are listed in Table 2 along with the cell parameters of the parent compounds ACo_2S_2 (A = K, Rb, Cs) for comparison. We observed an increase in the cell volume with increasing x in $KCo_{2-x}Cu_xS_2$. Similar results were also reported by Berger and Bruggen for the isostructural system $TlCu_{2-x}Fe_xSe_2$ (14).

The observed expansion of the a unit cell parameter on substitution for all members in the $ACo_{2-x}Cu_xS_2$ series (Table 2) ranges from ~0.15 Å (A = K) to ~0.2 Å (A = Rb, Cs). This change is not consistent with the ionic-size arguments, for the ionic radius of Cu^+ (0.74 Å) is very close to that of Co^{2+} (0.72 Å). The origin of the observed 3–6% increase in the a unit cell dimension compared with that of ACo_2S_2 appears to be electronic in nature.

A comparison of the c unit cell parameter of the quaternary phase $ACo_{2-x}Cu_xS_2$ with that of the ternary phase ACo_2S_2 (Table 2) shows that for the series $KCo_{2-x}Cu_xS_2$ (Table 2A) the difference is within the experimental error (~0.01Å). For the Rb and Cs phases (Table 2B), however, there are significant decreases of ~0.3 and ~0.7 Å, respectively, in the value of the c unit cell parameter when Cu replaces Co, possibly because the larger Rb^+ and Cs^+ ions better stabilize the layered structure than the smaller K^+ ion.

The A–S bonds in systems with the $ThCr_2Si_2$-type structure are considered to be almost purely ionic and the interlayer separation is determined by the effective ionic radius r_A of the alkali metal ion (C.N. = 8) (6). Therefore, in the order $KCoCuS_2$, $RbCoCuS_2$, $CsCoCuS_2$, the value of the c unit cell parameter increases linearly with r_A (Fig. 3), as expected.

In all of the reported AM_2S_2 ternary and quaternary chalcogenides with the $ThCr_2Si_2$-type structure, the $[M_2S_2]$ framework requires a large cation to form a stable structure (6). We are currently working on the synthesis of $ACoCuS_2$ sulfides (A = Li, Na). Not surprisingly $NaCoCuS_2$ adopts the trigonal (space group $P\bar{3}m1$) rather than the tetragonal $ThCr_2Si_2$-type structure. We also expect that $LiCoCuS_2$ should exist and form in this trigonal system. The isostructural compound $LiCuFeS_2$ has recently been reported (15). Investigations of the right experimental conditions for the formation of $LiCoCuS_2$ are in progress.

Transport Properties

Figure 4 shows the variation of resistivity with temperature in the system $KCo_{2-x}Cu_xS_2$ (x = 0.50, 0.60, 0.80, 1.00,

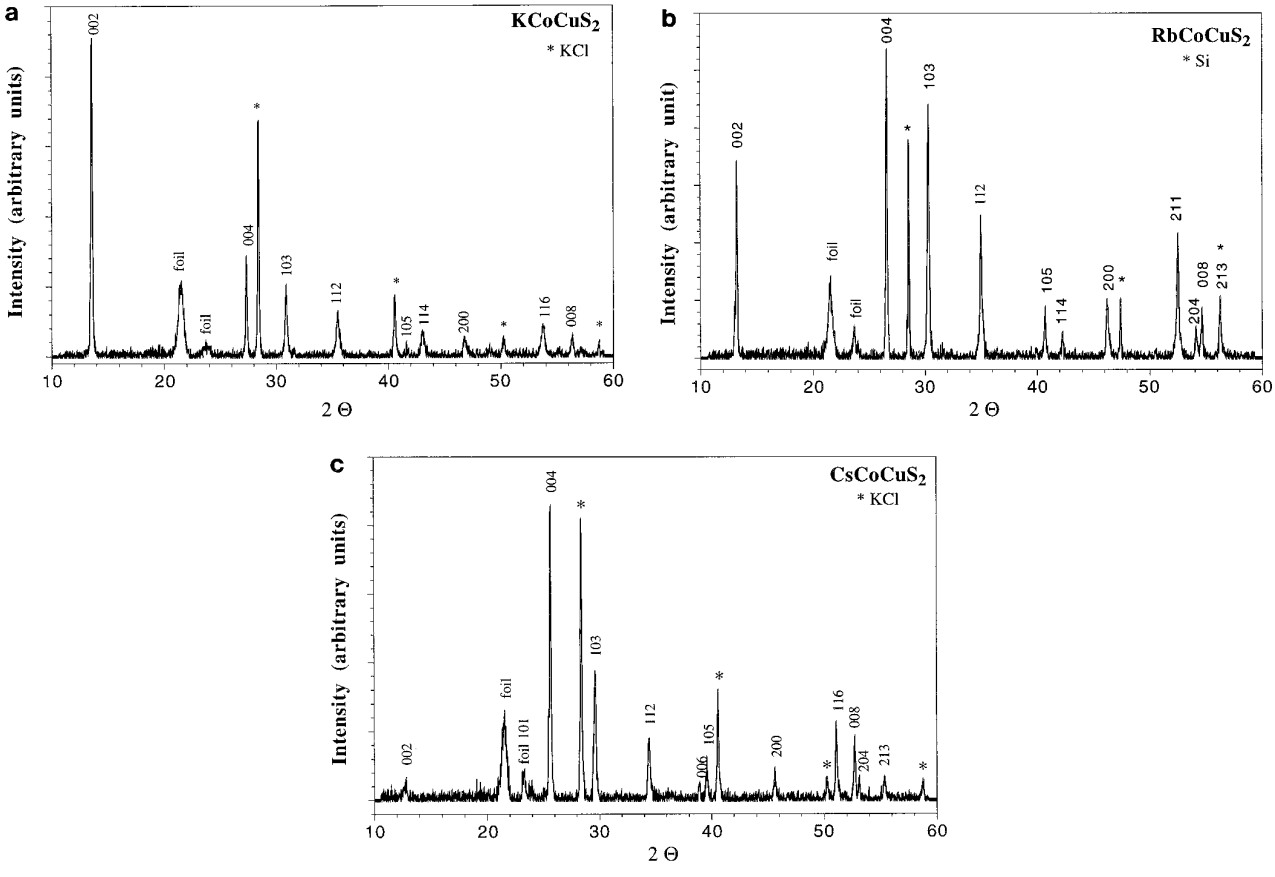

FIG. 2. (a) Typical powder X-ray diffraction pattern of the new quaternary sulfides $KCo_{2-x}Cu_xS_2$. (b) Powder X-ray diffraction pattern of $RbCoCuS_2$. (c) Powder X-ray diffraction pattern of $CsCoCuS_2$.

TABLE 2A
Unit Cell Parameters for $KCo_{2-x}Cu_xS_2$ Quaternary Sulfides

x	Composition	a (Å)	c (Å)	V (Å^3)
0.00	KCo_2S_2[a]	3.7298(5)	13.068(5)	181.79(6)
0.25	$KCo_{1.75}Cu_{0.25}S_2$[b]	3.88	13.05	196.4
0.50	$KCo_{1.50}Cu_{0.50}S_2$	3.8806(8)	13.064(2)	196.72(8)
0.60	$KCo_{1.40}Cu_{0.60}S_2$	3.8801(8)	13.065(2)	196.69(8)
0.70	$KCo_{1.30}Cu_{0.70}S_2$	3.8854(9)	13.081(2)	197.48(9)
0.75	$KCo_{1.25}Cu_{0.75}S_2$	3.8842(7)	13.071(2)	197.19(6)
0.80	$KCo_{1.20}Cu_{0.80}S_2$	3.889(1)	13.076	197.72(9)
0.90	$KCo_{1.10}Cu_{0.90}S_2$	3.886(1)	13.058(2)	197.2(1)
1.00	$KCoCuS_2$	3.8831(9)	13.058(1)	196.89(9)
1.20	$KCo_{0.80}Cu_{1.20}S_2$	3.876(1)	13.059(3)	196.22(9)
1.25	$KCo_{0.75}Cu_{1.25}S_2$	3.873(1)	13.057(3)	195.9(1)
1.30	$KCo_{0.70}Cu_{1.30}S_2$	3.872(2)	13.050(5)	195.7(2)
1.40	$KCo_{0.60}Cu_{1.40}S_2$	3.8729(7)	13.050(1)	195.74(7)
1.50	$KCo_{0.50}Cu_{1.50}S_2$	3.8693(9)	13.062(3)	195.56(9)
1.60	$KCo_{0.40}Cu_{1.60}S_2$[c]	3.862(2)	13.044(4)	194.6(2)

[a] After Ref. (6).
[b] Approximate values of unit cell parameters.
[c] Not a single phase (contains KCu_4S_3 phase).

TABLE 2B
Unit Cell Parameters for $ACoCuS_2$ (A = K, Rb, Cs) Quaternary Sulfides and for ACo_2S_2 Ternary Sulfides

Composition	a (Å)	c (Å)	c/a	V(Å^3)
$KCoCuS_2$	3.8831(9)	13.058(1)	3.363	196.89(9)
KCo_2S_2[a]	3.7298(5)	13.068(5)	3.504	181.79(6)
$RbCoCuS_2$	3.9314(5)	13.448(2)	3.421	207.85(6)
$RbCo_2S_2$[a]	3.725(2)	13.740(1)	3.689	190.7(2)
$CsCoCuS_2$	3.9667(9)	13.833(4)	3.487	217.66(9)
$CsCo_2S_2$[a]	3.736(2)	14.500(5)	3.881	202.4(2)

[a] After Ref. (6).

1.20, 1.40). There was no significant variation of the resistivity curves between heating and cooling cycles. The room temperature resistivities (ρ) and the thermal activation energies (E_a), as well as the a unit cell parameter of all the samples in this study, are summarized in Table 3.

Log(ρ) versus 1/T curves in Fig. 4 show that all of the samples presented here are degenerate semiconductors with small E_a values in the range 0.002 to 0.03 eV (Table 3). Only the sample that contains the largest amount of copper (i.e., "$KCo_{0.5}Cu_{1.5}S_2$") is metallic at room temperature and exhibits a broad metal-to-nonmetal transition at ~120 K (Fig. 5). Qualitative Seebeck coefficient measurements indicate that the primary charge carriers at room temperature are holes, independent of the value of x.

The schematic band diagrams for the end members of the series i.e., KCo_2S_2 and "KCu_2S_2," are presented in Figs. 6a and 6b, respectively. KCo_2S_2 is a n-type metal with an electrical conductivity of the order of 10^4 $(\Omega \cdot cm)^{-1}$ at room temperature (6). The metallic properties of KCo_2S_2 can be attributed to the presence of a partially filled conduction band as schematically shown in Fig. 6a. Although KCu_2S_2 has not been reported to date, it might exist as a metastable phase, isostructural with $TlCu_2S_2$, that also adopts $ThCr_2Si_2$-type structure. $TlCu_2S_2$ has been recently prepared and reported to be metastable and to decompose above 390 K (16). $TlCu_2S_2$ is a p-type metal, described by a charge formalism $Tl^+Cu_2^+S_2^{-1.5}$ (16). The metallic properties of $TlCu_2S_2$ are ascribed therefore to the presence of one hole per formula unit in a valence band, which is mainly sulfur 3p in character. Recent electronic band structure calculations of the $(Cu_{2n+1}S_{n+1})^-$ layers (n = 1, 2, 3) (17) pointed out that the important feature of the $Cu_2S_2^-$ layer is the presence of one hole per unit cell. The hole is located at the top of the valence band, which was found to be primarily Cu–S and Cu–Cu antibonding in character. The formation of $KCo_{2-x}Cu_xS_2$ compounds suggests that the potassium analog of $TlCu_2S_2$ (i.e., KCu_2S_2) should also

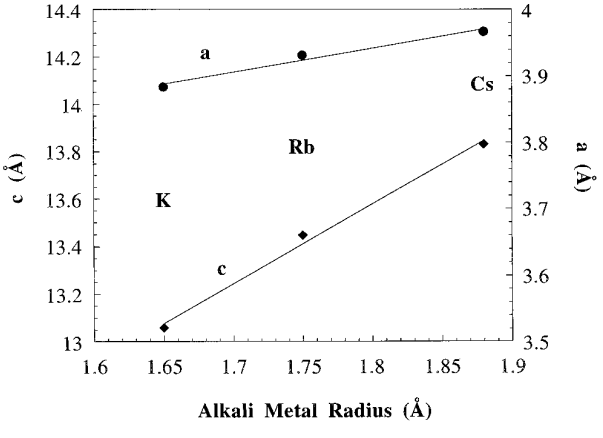

FIG. 3. Unit cell parameters as a function of the effective ionic radius of A for $ACoCuS_2$ (A = K, Rb, Cs).

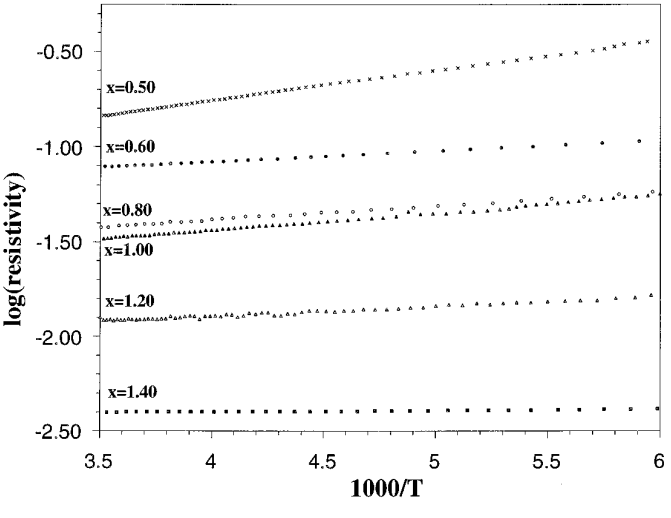

FIG. 4. Resistivity as a function of temperature for $KCo_{2-x}Cu_xS_2$ (x = 0.50, 0.60, 0.80, 1.00, 1.20, 1.40).

TABLE 3
Electrical Properties of $KCo_{2-x}Cu_xS_2$[a]

Composition	a(Å)	ρ_{RT} (10^{-2} Ω · cm)	Electrical behavior	E_a (eV) (200 K < T < 290 K)
0.50	3.8806(8)	14	Semiconductor	0.033
0.60	3.8801(8)	11	Semiconductor	0.011
0.80	3.889(1)	3.6	Semiconductor	0.015
1.00	3.8831(9)	3.2	Semiconductor	0.018
1.20	3.876(1)	1.2	Semiconductor	0.004
1.40	3.8729(7)	0.4	Semiconductor	0.002
1.50[b]	3.8693(9)	0.4	Metallic	—

[a] The error in the resistivity measurement is ±20%.
[b] Metal-to-nonmetal transition at ≈120 K.

exist as a metastable phase. The substitution of Cu ions by Co ions in this hypothetical "KCu_2S_2" appears to stabilize the $ThCr_2Si_2$-type structure, as evidenced by the formation of monophasic $KCo_{2-x}Cu_xS_2$ samples with $0.5 \leq x \leq 1.5$. With $x > 1.5$, the formation of structurally related KCu_4S_3 is favored at high temperature (i.e., 920 K). Our attempts to prepare "KCu_2S_2" by a CS_2/N_2 sulfurization method at 700 K, which seems to be the lowest temperature limit for this method, also yielded KCu_4S_3. These findings are consistent with the recent theoretical calculations that show the $Cu_4S_3^-$ layers to be somewhat more stable than the $Cu_2S_2^-$ layers (17). On the other hand, our preliminary results show that the synthetic route used successfully for the synthesis of $TlCu_2S_2$ (16) does not work in the case of "KCu_2S_2." $TlCu_2S_2$ was prepared from $TlCu_3S_2$ by immersing the latter in an aerated ammonia solution. The extraction of copper in the same manner from KCu_3S_2, however, does not result in the formation of KCu_2S_2, as evidenced by the PXD pattern of the reaction products. This is not surprising in view of instability of the K–Co–Cu–S system in air and moisture. Thus, the synthesis of "KCu_2S_2" requires alternate synthetic routes. The band structure of the hypothetical "KCu_2S_2" should be similar to that of $TlCu_2S_2$ (Fig. 6b) (p-type metal).

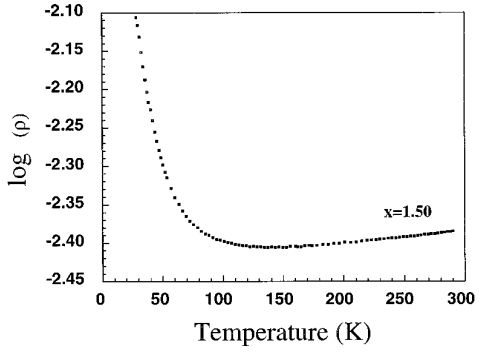

FIG. 5. Resistivity as a function of temperature for $KCo_{0.5}Cu_{1.5}S_2$.

Berger and Bruggen investigated $TlCu_2Se_2$ (18), which is isostructural with $ThCr_2Si_2$, and a series of solid-state solutions $TlCu_{2-x}Fe_xSe_2$ ($0 < x \leq 1$) (14) that have transport properties similar to those of $TlCu_2S_2$. In $TlCu_{2-x}Fe_xSe_2$, substitution of Cu^+ (d^{10}) by Fe^{3+} adds electrons into the valence band, reducing the number of the valence-band holes as well as the conductivity; compounds with $x \geq 0.5$ are semiconductors.

The sample with the highest copper content that could be prepared by us that has the nominal composition $KCo_{0.5}Cu_{1.5}S_2$ is metallic down to ~120 K, where it exhibits a metal-to-nonmetal transition. Because copper generally is considered to be monovalent in sulfides (19–21), and cobalt in this phase is most probably trivalent (i.e., $K^+Co^{3+}_{0.5}Cu^+_{1.5}S^{2-}_2$), semiconducting properties should be expected. The actual composition of this phase, however, corresponds to $K_{0.96}Co_{0.53}Cu_{1.50}S_{2.14}$ (Table 1). The oxidation formalism $[(K^+)_{0.96}(Co^{3+})_{0.53}(Cu^+)_{1.50}(S^{2-})_{2.14}]$ indicates that there are holes at the top of the valence band (Fig. 6c) and that the small deviation from stoichiometry has a pronounced effect on the electrical properties in this case.

The phases $KCo_{2-x}Cu_xS_2$ with $1.0 < x < 1.5$ are degenerate semiconductors with very small E_a values corresponding most probably to a partially filled narrow band of Co^{2+} parentage, which becomes filled for $x = 1$ (Fig. 6d).

On the other hand, the semiconducting properties of the "cobalt-rich" part of the system $KCo_{2-x}Cu_xS_2$ ($0.5 \leq x \leq 1.0$) may be correlated with several factors, two of which seem to be especially important:

1. the disruption of the electronic correlations between cobalt ions within a layer, on the random substitution by copper ions; and
2. the change of the a unit cell parameter on substitution of cobalt ions by copper ions.

The introduction of copper ions, as a quaternary element, modifies the energy band diagram of the ternary

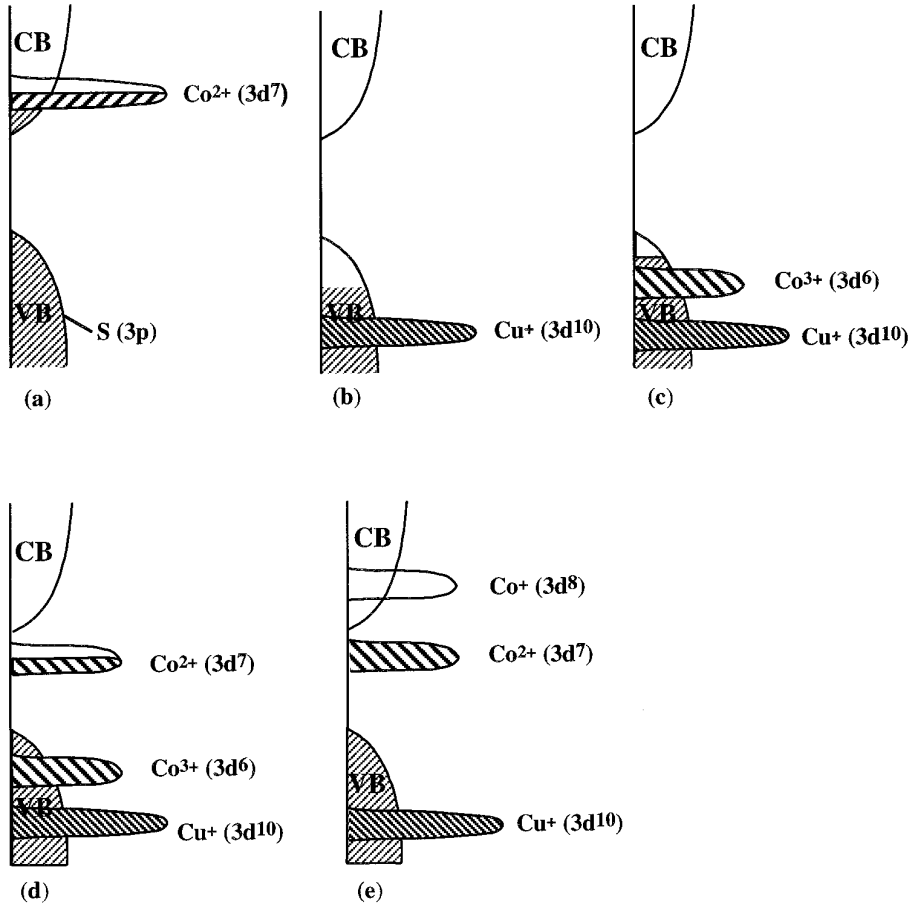

FIG. 6. Schematic energy band diagrams E versus $N(E)$ of (a) KCo_2S_2, (b) $TlCu_2S_2$, (c) $KCo_{2-x}Cu_xS_2$ ($x = 1.5$), (d) $KCo_{2-x}Cu_xS_2$ ($1.0 \leq x < 1.5$), (e) $KCo_{2-x}Cu_xS_2$ ($0.5 \leq x < 1$) [see Refs. (19, 21)].

KCo_2S_2. The schematic energy band diagram of the ''cobalt-rich'' part of the quaternary $KCo_{2-x}Cu_xS_2$ system ($x < 1$) is shown in Fig. 6e. The observed semiconducting properties can be explained by the presence of a gap between a filled narrow band formed by the overlap of cobalt d orbitals and an empty conduction band. That the origin of semiconducting behavior is not due to variable hopping of electrons in a partially filled narrow band has been confirmed by the linear behavior of $\log(\rho)$ versus $1/T$ plots [i.e., $\log(\rho)$ versus $1/T^{1/4}$ is linear for variable hopping mechanism].

The a unit cell parameter corresponds to the length of the edge of the MS_4 tetrahedra. An increase in the MS_4 tetrahedral length in $KCo_{2-x}Cu_xS_2$ of ~0.1 Å, when compared with ternary KCo_2S_2 (Table 2), leads to an increase in the metal–metal distance and, thus, to a weakening of metal–metal orbital overlap, which in turn may explain the absence of metallic properties in $KCo_{2-x}Cu_xS_2$. As Table 3 shows, for the ''cobalt-rich'' phases, i.e., in $KCo_{2-x}Cu_xS_2$ with $0.5 \leq x < 1.0$, the a unit cell parameter is ~3.88 Å, and the corresponding room temperature resistivities are of comparable order of magnitude. For $x > 1$ in $KCo_{2-x}Cu_xS_2$, (the ''copper-rich'' part of the system) the a unit cell parameter decreases as do the resistivities. The observed decrease in the a unit cell parameter and the resistivity is consistent with the energy band diagram, which for the ''copper-rich'' part of the $KCo_{2-x}Cu_xS_2$ system resembles more that of the hypothetical ''KCu_2S_2'' ($TlCu_2S_2$) (Fig. 6b) than that of KCo_2S_2 (Fig. 6a). The energy band diagram of the ''cobalt-rich'' part of the system ($0.5 \leq x < 1$) in this study is more like that of KCo_2S_2.

The above discussion on the transport properties of $KCo_{2-x}Cu_xS_2$ can also be extended to $RbCoCuS_2$ and $CsCoCuS_2$. As seen in Fig. 7 and Table 4, the replacement of potassium ion by a larger alkali metal ion did not significantly change either the resistivity or the activation energy.

Magnetic Properties

The variation of the inverse magnetic susceptibility as a function of temperature for the three $ACoCuS_2$ (A =

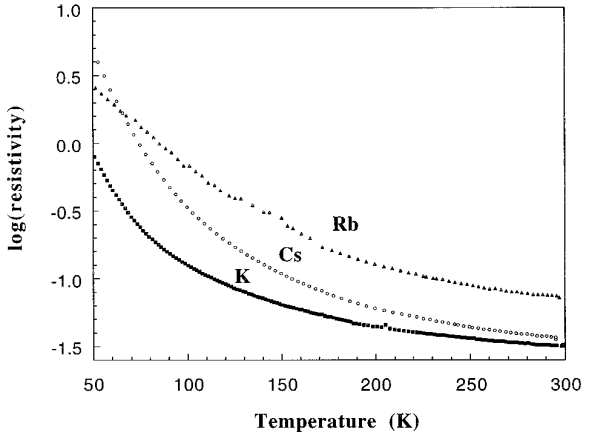

FIG. 7. Resistivity as a function of temperature for ACoCuS$_2$ (A = K, Rb, Cs).

K, Rb, Cs) phases, prepared under similar experimental conditions, is presented in Fig. 8. The magnetic susceptibilities of these compositions at room temperature, corrected for the diamagnetism of the core atoms, are listed in Table 5. The large paramagnetic moment observed in all three samples is indicative of the presence of localized moments. These local moments are assumed to be associated with the cobalt ions, since the alkali metal ions carry no unpaired electrons and the copper, as already indicated, is considered to be monovalent (d^{10}) in sulfides (19–21).

As can be seen from Fig. 8, regardless of the nature of the A ion, all three phases undergo a transition to a ferromagnetic state with a Curie temperature $T_c \sim 120$ K. Unlike the classical ferromagnets, where the temperature variation of the magnetic susceptibility can be fit to a Curie–Weiss law in a temperature range well above T_c, the ACoCuS$_2$ compositions studied here clearly display a complex behavior. For example, the temperature dependence of the susceptibility above T_c for all the samples suggests antiferromagnetic exchange correlations (i.e., the Weiss constant is large and negative), although a transition observed near 120 K is ferromagnetic in character. Likewise, the apparently similar values of T_c observed for all the compositions are in contrast with similar studies on ACo$_2$S$_2$ phases where T_c was shown to be sensitive to the size of the A cation located between the layers. To explain the observed anomalous magnetic behavior, three possible effects were considered: (1) ferromagnetic impurities, (2) ferrimagnetism, and (3) anisotropic magnetic exchange interactions.

Detailed field-dependent magnetization studies at different temperatures were carried out to verify the presence of saturated magnetization associated with possible ferromagnetic impurities. In all the measurements, the magnetization increased linearly with the applied magnetic field at temperatures above T_c, indicating the absence of ferromagnetic impurities. Ferrimagnetic interactions, on the other hand, require the presence of two magnetic sublattices in which the magnetic ions occupy different crystallographic sites. From the earlier discussion of the structural aspects, it is known that all the magnetic ions (in this case the Co ions) occupy identical crystallographic sites. That implies that the ferrimagnetism is unlikely to occur.

Recently Huan *et al.* (22) have demonstrated by powder neutron diffraction and oriented single-crystal magnetization studies that for TlCo_2X_2 (X = S, Se) phases, which are isostructural with ACoCuS$_2$, the in-plane (i.e., the *ab* plane) exchange interactions are ferromagnetic, while those along the *c* axis are ferromagnetic when X = S and antiferromagnetic when X = Se. In view of the structural similarities between TlCo_2X_2 and ACoCuS$_2$, it appears likely that the magnetic correlations are similar in these phases. Surprisingly, however, the observed magnetic behavior of ACoCuS$_2$ phases seems to resemble that of TlCo_2Se_2 rather than that of TlCo_2S_2. Thus, the magnetic susceptibility above T_c is likely dominated by the *c*-axis interactions, accounting for the observed negative Weiss constant, whereas near and below T_c, the in-plane interactions may be strong enough to make the overall order ferromagnetic. Furthermore, the contrasting behavior observed in the T_c dependence on the size of the A-site cation in ACo$_2$S$_2$ and ACoCuS$_2$ compositions can be related to the *c*/*a* ratios (Table 2B). For the ACo$_2$S$_2$ system the variation in *c*/*a* with the size of the A cation is more pronounced than for the ACoCuS$_2$ system (6). For example the difference in the value of the *c*/*a* ratio between RbCo$_2$S$_2$ and KCo$_2$S$_2$ is ≈0.19 Å, whereas the same difference between

TABLE 4
Electrical Properties of ACoCuS$_2$ (A = K, Rb, Cs)[a]

Composition	a(Å)	ρ_{RT} (10^{-2} Ω · cm)	Electrical behavior	E_a (eV) (200 K < T < 290 K)
KCoCuS$_2$	3.8831(9)	3.2	Semiconductor	0.018
RbCoCuS$_2$	3.9314(5)	7.5	Semiconductor	0.029
CsCoCuS$_2$	3.9667(9)	3.6	Semiconductor	0.016

[a] The error in the resistivity measurement is ±20%.

TABLE 5
Room Temperature Magnetic Susceptibility and T_c for $ACoCuS_2$ (A = K, Rb, Cs) and for ACo_2S_2[a]

Composition	T_c (K)	χ(RT) (10^{-3} emu/mol)
$KCoCuS_2$ (KCo_2S_2)	120 (127)	2.8 (4.3)
$RbCoCuS_2$ ($RbCo_2S_2$)	120 (87)	3.0 (3.7)
$CsCoCuS_2$ ($CsCo_2S_2$)	120 (70)	2.7 (2.6)

[a] After Ref. (6). Applied magnetic field 1000 G.

corresponding quaternary $RbCoCuS_2$ and $KCoCuS_2$ phases is ≈0.06 Å. Likewise the difference between $CsCo_2S_2$ and $RbCo_2S_2$ is also ≈0.19 Å; however, the difference between $CsCoCuS_2$ and $RbCoCuS_2$ is only about ≈0.06 Å. Therefore, the T_c in these systems is sensitive to the c/a value.

Finally, we would like to point out that the magnetic properties of the samples investigated here are sensitive to their thermal history and synthetic conditions. To illustrate this effect two samples of $KCoCuS_2$ were prepared: one at 720°C and the other at 900°C. Although both specimen are pure (by PXD), their temperature-dependent magnetizations (Fig. 9) are clearly different. The sample prepared at lower temperature displays higher magnetic susceptibilities and a higher T_c (~120 K; Fig. 9a) than the sample prepared at higher temperature (T_c ~ 50 K; Fig. 9b). The observed dependency of the magnetic properties on the synthetic conditions may be attributed to differences in the distribution of Co and Cu ions and/or sulfur deficiency in the products.

CONCLUSION

Single-phase polycrystalline quaternary sulfides with the formulas: $ACoCuS_2$ (where A = K, Rb, Cs) and $KCo_{2-x}Cu_xS_2$ ($0.5 \le x \le 1.5$) have been prepared for the first time by sulfurization of a mixture of the corresponding alkali metal carbonate, copper oxide, and cobalt oxide precursors in a stream of CS_2 carried by N_2 at temperatures between 650 and 900°C.

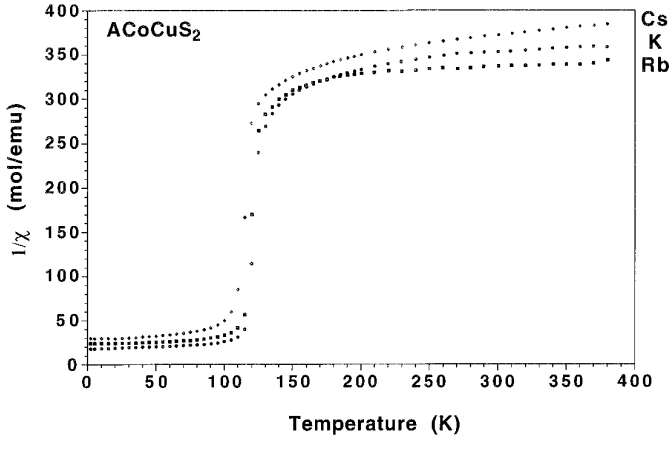

FIG. 8. Inverse magnetic susceptibility $1/\chi$ as a function of temperature for $ACoCuS_2$ (A = K, Rb, Cs); the applied field is 1000 G.

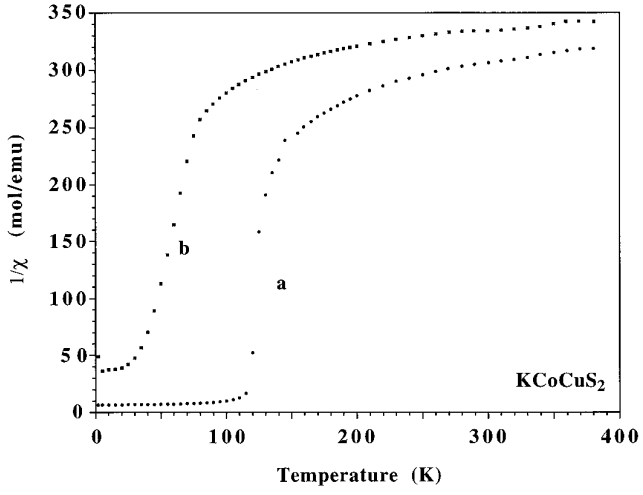

FIG. 9. Inverse magnetic susceptibility $1/\chi$ as a function of temperature for $KCoCuS_2$ prepared at 720°C (a) and 900°C (b); the applied field is 1000 G.

Electrical resistivity measurements show that all the samples except $KCo_{0.5}Cu_{1.5}S_2$ are p-type degenerate semiconductors with relatively high conductivities at room temperature ($\rho_{RT} \sim 10^{-2}\ \Omega \cdot$ cm) and very small activation energies in the range 0.002 to 0.03 eV. $KCo_{0.5}Cu_{1.5}S_2$ is a p-type metal and exhibits a broad metal-to-nonmetal transition at ~120 K. The metallic behavior is attributed to the presence of holes at the top of the valence band.

The observed transport properties of the $KCo_{2-x}Cu_xS_2$ ($0.5 \le x \le 1.5$) phases have been interpreted in terms of schematic band diagrams derived from those of the end members, KCo_2S_2 and "KCu_2S_2." Replacement of the potassium ion with a larger alkali metal ion in $ACoCuS_2$ (A = Rb, Cs) did not significantly change either the resistivity or the activation energy of the compounds.

The magnetic data for the three phases $ACoCuS_2$ (A = K, Rb, Cs) indicate an anomalous transition to a ferromagnetic state at $T_c \sim 120$ K and strong antiferromagnetic interactions well above T_c. The complex magnetic behavior observed may be attributed to anisotropic magnetic exchange interactions: ferromagnetic in the ab plane and antiferromagnetic along the c axis. The magnitude of the net 3D magnetic moment is determined by competing exchange interactions and the c/a value is an important factor. Because in $ACoCuS_2$ the c/a values are similar, the T_cs for different As are nearly identical.

ACKNOWLEDGMENTS

We thank Professor Bill McCarroll for critically reading this manuscript. Dr. P. Höhn is acknowledged for useful discussions. One of us

(K.V.R.) thanks Rowan College for the award of PAG release time. This work was supported by the National Science Foundation under Solid State Chemistry Grant DMR-93-14605.

REFERENCES

1. W. B. Pearson, *J. Solid State Chem.* **56,** 278 (1985).
2. K. Klepp and H. Boller, *Monatsch. Chim.* **109,** 1049 (1978).
3. L. W. Haar, F. J. DiSalvo, H. E. Bair, R. M. Fleming, and J. V. Waszczak, *Phys. Rev. B* **35,** 1932 (1987).
4. J. Etourneau, in ''Solid State Chemistry'' (P.D. A.K. Cheetham, Ed.), p. 60. Clarendon, Oxford, 1992.
5. R. Hoffmann and C. Zhong, *J. Phys. Chem.* **89,** 4174 (1985).
6. G. Huan, M. Greenblatt, and M. Croft, *Eur. J. Solid State Inorg. Chem.* **26,** 193 (1989).
7. C. Mujica, J. Paez, and J. Lianos, *Mater. Res. Bull.* **29,** 263 (1994).
8. D. Schmitz and W. Bronger, *Z. Anorg. Allg. Chem.* **248,** 248 (1987).
9. A. J. Jacobson and L.E. McCandlish, *J. Solid State Chem.* **29,** 355 (1979).
10. T. H. Geballe, *Science* **259,** 1550 (1993).
11. B. W. Eichhorn, *in* ''Progress in Inorganic Chemistry'' (K. D. Karlin, Eds.), p. 139. Wiley, New York, 1994.
12. M. Dobrovolskaya, W. P. Rogova, A. I. Celin, and W. Malov, *Zap. Vses. Mineral. O-va*. **110,** 468 (1980).
13. K. Klepp, H. Boller, and H. Vollenkle, *Monatsch. Chem.* **111,** 727 (1980).
14. R. Berger and C. F. v. Bruggen, *J. Less-Common Met.* **113,** 291–323 (1985).
15. R. Fong, J. R. Dahn, R. J. Batchelor, F. W. B. Einstein, and C. H. W. Jones, *Phys. Rev. B* **39,** 4424 (1989).
16. R. Berger, *J. Less-Common Met.* **147,** 141 (1989).
17. G. V. Vajenine and R. Hoffmann, *Inorg. Chem.*, 451 (1996).
18. R. Berger and C. F. v. Bruggen, *J. Less-Common Met.* **99,** 113 (1984).
19. F. Jellinek, *in* ''Inorganic Sulfur Chemistry'' (G. Nickless, Ed.). Elsevier, Amsterdam/London/New York, 1968.
20. J. C. W. Folmer and F. Jellinek, *J. Less-Common Met.* **76,** 153 (1980).
21. C. F. v. Bruggen, *Ann. Chim. Fr.* **7,** 171 (1982).
22. G. Huan, M. Greenblatt, and K. V. Ramanujachary, *Solid State Commun.* **71,** 221 (1989).